Biomech Model Mechanobiol
DOI 10.1007/s10237-013-0478-z

ORIGINAL PAPER

The stretching elasticity of biomembranes determines their line tension and bending rigidity

Luca Deseri · Giuseppe Zurlo

Received: 23 October 2012 / Accepted: 13 February 2013

Abstract In this work, some implications of a recent model for the mechanical behavior of biological membranes (Deseri et al. in Continuum Mech Thermodyn 20(5):255–273, 2008) are exploited by means of a prototypical one-dimensional problem. We show that the knowledge of the membrane stretching elasticity permits to establish a precise connection among surface tension, bending rigidities and line tension during phase transition phenomena. For a specific choice of the stretching energy density, we evaluate these quantities in a membrane with coexistent fluid phases, showing a satisfactory comparison with the available experimental measurements. Finally, we determine the thickness profile inside the boundary layer where the order–disorder transition is observed.

Keywords Biomembranes · Lipid bilayers · Phase transitions · Line tension · Bending rigidity · Stretching elasticity

1 Introduction

The mechanical behavior of biological membranes is regulated by the interaction of a very rich list of features, such as their elastic properties, their chemical composition, and their capability of undergoing ordering–disordering phenomena. It is also well known that their special constitutive nature enables them to sustain bending moments but not in-plane shear stresses (unless their viscosity is accounted for).

The resulting effects of this interaction are evidenced by a wide variety of configurations that can be maintained by biological membranes at equilibrium for given values of overall chemical composition, controlled temperature, or applied osmotic pressure (Bermúdez et al. 2004; Das et al. 2008; Iglic 2012; Sackmann 1995).

In the last decade, the growing availability of advanced microscopy and imaging techniques has led to a blooming of interest in the study of biological membranes, revealing often spectacular examples of the intricate interplay of the various features characterizing their behavior (see, e.g., Baumgart et al. 2003).

The main literature on the modeling of the mechanical behavior of biological membranes can be traced back to the pioneering works of Canham (1970) and Helfrich (1973), who derived elastic models describing the bending behavior of *lipid bilayers*, the building blocks of all types of biological membranes. These and similar models of the bilayer bending elasticity have been fruitfully exploited in the literature for the study of equilibrium shapes of biomembranes, including red blood cells (Canham 1970; Jenkins 1977), the effects of embedded proteins or rod-like inclusions (Agrawal and Steigmann 2009; Biscari and Bisi 2002), and the analysis of phase transition phenomena leading to the formation of buds (Lipowsky 1992), with the possible coexistence of phase domains characterized by different bending rigidities (Agrawal and Steigmann 2008; Baumgart et al. 2005).

Aside from the study of the bending properties of such structures, a significant area in the literature on biomembranes is devoted to the analysis of the order–disorder transition in planar lipid bilayers (Akimov et al. 2003;

L. Deseri
Center for Nonlinear Analysis and Department of Mathematical Sciences, Carnegie Mellon University, Pittsburgh, PA 15213-3890, USA
e-mail: deseri@andrew.cmu.edu

G. Zurlo (✉)
Marie Curie Fellow of the Istituto Nazionale di Alta Matematica "Francesco Severi", Laboratoire de Mécanique des Solides—École Polytechnique, 91128 Palaiseau Cedex, France
e-mail: g.zurlo@poliba.it

Published online: 05 March 2013

Chen et al. 2001; Goldstein and Leibler 1989; Iglic 2012; Owicki and McConnell 1979) and to the effects of special molecules (such as cholesterol) in relation to this type of transition (Komura et al. 2004; Pan et al. 2009; Rawicz et al. 2000). Within this framework, a remarkable issue is the analysis of line tension at the boundary of ordered–disordered domains: It is now recognized that, together with bending rigidities, line tension plays a major role in maintaining non-spherical configurations observed in experiments (Akimov et al. 2003; Honerkamp-Smith et al. 2008; Lipowsky 1992; Trejo and Ben Amar 2011).

In the effort of deducing a unitary model of biomembranes where their elastic behavior, their possibility of undergoing ordering–disordering phenomena, and their chemical composition are consistently taken in consideration, in Deseri et al. (2008), Zurlo (2006) the expression of the energy regulating the thermo–chemo–mechanical behavior of biological membranes was derived, within the framework of a formal asymptotic 3D-to-2D reduction, based on thinness assumptions. This procedure can be generalized by means of a dimension reduction of an elastic energy accounting for the submacroscopic structure (Deseri and Owen 2010). A rigorous derivation of the two-dimensional energy of biomembranes undergoing large deformations from their three-dimensional properties is currently in preparation (Deseri et al). Analogous efforts in order to extract an areal energy density from the three-dimensional energy density of a bilayer endowed with nonvanishing spontaneous curvature have been recently carried out by Maleki et al. (2012).

The model proposed in Deseri et al. (2008), Zurlo (2006), here summarized in Sect. 2, reveals the possibility of describing the geometrical (shape) and conformational (state of order) behavior of the lipid bilayer on the basis of one single ingredient: the in-plane membrane stretching elasticity, regulating the material response with respect to local surface dilatations. A rigorous analysis of coexistent fluid-phase membranes, endowed of an energy density obtainable from the one deduced in Deseri et al. (2008), is carried out by Choksi et al. (2012).

In essence, the major point in Deseri et al. (2008), Zurlo (2006) is that the bilayer stretching elasticity is enough to describe its order–disorder transition (together with the influence of chemical composition), to determine the profile and the length of the boundary layer where the membrane thickness passes from a thicker domain (ordered phase) to a thinner one (disordered phase), to evaluate the corresponding line tension and finally to determine the bending rigidities in both phases.

Here, in order to elucidate the feasibility of this model, a prototypical planar problem has been studied. On the basis of a specific Landau expansion of the stretching energy density—calibrated on the basis of the experimental estimates provided by Goldstein and Leibler (1989)—the line tension, the thickness profile inside the boundary layer, and the area compressibility and bending moduli are calculated, showing a satisfactory agreement with the data known in the experimental and theoretical literature. In order to keep the analysis as simple as possible, here we confine our attention to a planar patch of membrane, although we remark that the issues discussed in this work play a crucial role in the out-of-plane behavior of membranes undergoing phase transition phenomena: These issues will be further discussed in future papers.

In this work, we illustrate how, by making use of the results obtained in Deseri et al. (2008), Zurlo (2006), it is possible to establish a precise connection among several features of lipid bilayers: line tension, area compressibility modulus, bending moduli, and order–disorder transition zone. Furthermore, we establish a link among these features and measurable quantities, such as the transition temperature, the latent heat, and the thickness difference at the order–disorder transition. We believe that elucidating these connections moves a significant step forward toward understanding the complex phenomena taking place in biological membranes.

The approach originally proposed in Deseri et al. (2008), Zurlo (2006) can be easily extended in order to consider the effects of spontaneous curvature and the effects arising from the presence of electric charges on the inner and outer membrane surfaces (Puglisi and Zurlo 2012), which play a fundamental role on the stability of thin elastic membranes (De Tommasi et al. 2011, 2012, 2013b). Further studies of the dynamics of moving phase boundaries and of the role of the line tension may be performed by following the path traced in Deseri and Owen (2012). These issues will be discussed in a series of forthcoming papers.

2 Summary of the model

In this section, we briefly recall the main results obtained in Deseri et al. (2008), Zurlo (2006), together with a schematic description of the approach followed in these works. The main result is the derivation of a new surface energy density for the lipid bilayer, building block of all biomembranes, which gives the possibility of deducing bending rigidities, line tension, and thickness profile inside the boundary layer during the order–disorder transition from simple experimental data on the stretching behavior of the membrane.

In Deseri et al. (2008), Zurlo (2006), attention was restricted to initially planar membranes, that is, spontaneous curvature has been neglected: This issue will be discussed in a forthcoming paper.

Introduce an orthonormal reference frame $(\boldsymbol{e}_1, \boldsymbol{e}_2, \boldsymbol{e}_3)$ and assume that the reference configuration of the membrane is a prismatic region $\mathscr{B}_0$ of constant thickness h_0 in direction $\boldsymbol{e}_3$ and with a flat mid-surface Ω in the plane spanned by

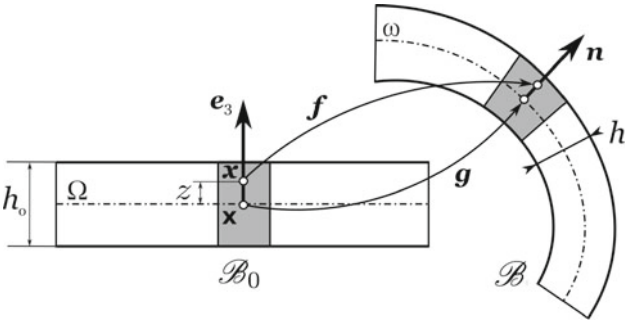

Fig. 1 Schematic representation of the deformation (4) of a prismatic, plate-like reference configuration $\mathscr{B}_0$ into the current configuration $\mathscr{B}$. The *gray box* depicts the space occupied by two lipid molecules, their volume being conserved during the deformation

$(\boldsymbol{e}_1, \boldsymbol{e}_2)$. Points of $\mathscr{B}_0$ are denoted by

$$\boldsymbol{x} = \mathbf{x} + z\boldsymbol{e}_3, \tag{1}$$

where $\mathbf{x} = x\boldsymbol{e}_1 + y\boldsymbol{e}_2$ and $z \in (-h_0/2, h_0/2)$. Denote by $\boldsymbol{f}$ the deformation map of $\mathscr{B}_0$ and by $\mathbf{F} = \nabla \boldsymbol{f}$ the deformation gradient. Thus, the stored Helmholtz energy can be expressed as

$$\mathscr{E}(\boldsymbol{f}) = \int_{\mathscr{B}_0} W(\mathbf{F})\,\mathrm{d}V = \int_{\Omega}\int_{-h_0/2}^{h_0/2} W(\mathbf{F})\,\mathrm{d}z\,\mathrm{d}\Omega, \tag{2}$$

where W is the purely elastic Helmholtz energy density. The surface energy density is, then,

$$\psi(\boldsymbol{f}) = \int_{-h_0/2}^{h_0/2} W(\mathbf{F})\,\mathrm{d}z. \tag{3}$$

Biological membranes of interest for this work are characterized by the so-called *in-plane fluidity*, corresponding to the impossibility of sustaining shear stresses in planes perpendicular to $\boldsymbol{e}_3$, unless some viscosity is present. This constitutive assumption can be used to restrict the point-wise dependence of the Helmholtz energy density W on a suitable list of three invariants of $\mathbf{C} = C_{ij}\boldsymbol{e}_i \otimes \boldsymbol{e}_j = \mathbf{F}^T\mathbf{F}$, $(i, j = 1, 2, 3)$ (see Deseri et al. for the proof),

$$\begin{aligned}
\eta_1(\boldsymbol{x}) &= \det[C_{\alpha\beta}(\boldsymbol{x})],\\
\eta_2(\boldsymbol{x}) &= C_{33}(\boldsymbol{x}),\\
\eta_3(\boldsymbol{x}) &= \det \mathbf{C}_(\boldsymbol{x}),
\end{aligned}$$

where $\alpha, \beta = 1, 2$ and where $C_{33} = \mathbf{C}\boldsymbol{e}_3\cdot\boldsymbol{e}_3$. The kinematical interpretation of these three invariants shows that $\sqrt{\eta_1}$ is the areal stretch of planes perpendicular to the direction $\boldsymbol{e}_3$, $\sqrt{\eta_2}$ is the stretch in direction $\boldsymbol{e}_3$, and $\sqrt{\eta_3}$ is the variation of volume.

In order to capture the out-of-plane deformations of the membrane and the occurrence of inhomogeneous thickness deformations, we restrict the membrane kinematics by the following *ansatz* (see Fig. 1)

$$\boldsymbol{f}(\boldsymbol{x}) = \boldsymbol{g}(\mathbf{x}) + z\phi(\mathbf{x})\boldsymbol{n}(\mathbf{x}), \tag{4}$$

where the map $\boldsymbol{g}(\mathbf{x})$ defines the position of the current mid-surface of the membrane $\omega = \boldsymbol{g}(\Omega)$, where $\boldsymbol{n}$ is the outward normal to ω and where $\phi(\mathbf{x}) = h(\mathbf{x})/h_0$ is the thickness stretch, with h the current thickness. This ansatz permits to make explicit the dependence of the invariants $\eta_i\,(i = 1, 2, 3)$ on the variable z so that, after the explicit integration (3), it is finally possible to perform the expansion of the surface energy density $\psi(\boldsymbol{f})$ in powers of the reference thickness h_0.

As matter of fact, this expression can be further simplified on the basis of the substantial bulk incompressibility of the lipid molecules. Indeed, let the gray area in Fig. 1 to represent the volume occupied by a cluster of lipid molecules: The experimental evidence (Goldstein and Leibler 1989; Owicki and McConnell 1979) suggests that the molecular volume of biological membranes can be considered constant in a wide range of temperature. Consistently with the ansatz (4), this condition can be imposed by means of a *quasi-incompressibility* constraint

$$\det \mathbf{C}(\mathbf{x}, 0) = \eta_1(\mathbf{x}, 0)\eta_2(\mathbf{x}, 0) = 1 \quad \text{for all } \mathbf{x} \in \Omega. \tag{5}$$

For a general deformation $\boldsymbol{g}$, the constraint (5) expresses a first-order approximation in the variable z of the exact incompressibility constraint $\eta_3 = 1$. Nevertheless, if the membrane undergoes a plane deformation, so that $\omega = \boldsymbol{g}(\Omega)$ is contained in the plane $z = 0$, the condition (5) coincides with the exact incompressibility constraint (see details in Deseri et al. 2008). This is the special case taken in consideration in this work.

These positions motivate the introduction of a restriction of the Helmholtz energy density W to Ω in the class of quasi-incompressible deformations,

$$w(J) = W(\eta_1, \eta_2, \eta_3)\Big|_{z=0} = W(J^2, J^{-2}, 1), \tag{6}$$

where we have set

$$J(\mathbf{x}) = \sqrt{\eta_1(\mathbf{x}, 0)}, \tag{7}$$

which can be interpreted as the areal stretch of the mid-surface Ω. With these settings, the quasi-incompressibility constraint takes the form $\phi J = 1$.

Under the ansatz (4), under the assumptions of in-plane fluidity and bulk quasi-incompressibility, the thickness expansion of (3) up to h_0^3 finally gives the main result obtained in Deseri et al. (2008), Zurlo (2006), that is, the expression of the surface energy density of a lipid bilayer undergoing inhomogeneous thickness deformations,

$$\psi = \varphi(J) + \kappa(J)H^2 + \kappa_G(J)K + \alpha(J)||\mathrm{grad}_\omega \widehat{J}||^2, \tag{8}$$

where H and K are, respectively, the mean and Gaussian curvatures of the mid-surface ω, where

$$\varphi(J) = h_0\, w(J) \tag{9}$$

can be interpreted as the first-order, *stretching* energy density of the membrane and where the bending rigidities amount to

$$k(J) = \frac{h_0^2}{6}\varphi''(J), \quad k_G(J) = \frac{h_0^2}{12J}\varphi'(J), \tag{10}$$

where $' = d/dJ$. The last term in (8) is a penalty for spatial changes of J. Here, $\widehat{J}$ is the spatial description of J, defined by the composition $\widehat{J} \circ \boldsymbol{g} = J$, and grad_ω is the gradient with respect to points of the current mid-surface ω; the penalty modulus is

$$\alpha(J) = \frac{h_0^2}{24J^3}\varphi'(J). \tag{11}$$

Classically, the bending energy is expressed in terms of the current surface ω rather than on the reference surface Ω, so that it makes sense to define the bending rigidities on the current configuration (see, e.g., Baumgart et al. 2003)

$$\kappa(J) = \frac{h_0^2}{6J}\varphi''(J), \quad \kappa_G(J) = \frac{h_0^2}{12J^2}\varphi'(J). \tag{12}$$

Observe that, as expected from thin shells elasticity (see, e.g., Norouzi et al. 2006), both the bending rigidities k, k_G are of order h_0^3.

The expression (8) is consistent with several models previously introduced in the literature of biological membranes. For a curved membrane with J fixed, it results (up to a constant) that $\psi = kH^2 + k_G K$, which is the well-known bending Helfrich energy density for lipid bilayer membranes (Helfrich 1973). For a flat membrane ($H = K = 0$) with thickness inhomogeneities, the surface energy density (8) is reminiscent of the asymptotic model deduced by Coleman and Newman (see, e.g., Coleman and Newman 1988) for the cold drawing of thin polymeric rods and films. Also, without the nonlocal term $\alpha(J)||\text{grad}_\omega \hat{J}||^2$ and without the explicit knowledge of the bending rigidities, it coincides with the energy determined in Baesu et al. (2004).

The analysis carried out in this work is based on several simplifying assumptions, both regarding the membrane kinematics and its constitutive behavior. For example, we observe that a finer description of the lipid kinematics requires the possibility of describing the so-called *tilt* deformations, corresponding to deviations from the normality preserving condition (Akimov et al. 2003; Hamm and Kozlov 2000). Here we neglect this type of deformations, which would require a richer kinematics than the one represented by (4), possibly by making use of structured deformations (see, e.g., Deseri and Owen 2003, 2012). Nevertheless, we point out that the approach followed in Deseri et al. (2008), Zurlo (2006) can be easily generalized in order to account for more general constitutive assumptions, for chemical composition, temperature dependence, and for the presence of spontaneous curvature.

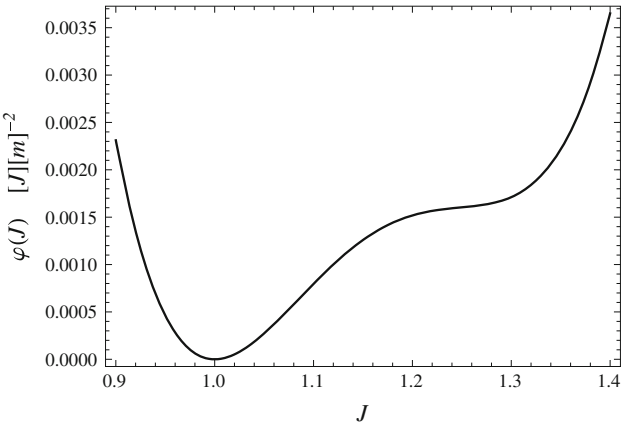

Fig. 2 The stretching energy $\varphi(J)$ adapted from Goldstein and Leibler (1989), for a temperature $T \sim 30°$. The areal stretch $J_o = 1$ corresponds to the unstressed, reference configuration $\mathscr{B}_0$

3 Stretching energy

The main ingredient of the two-dimensional membrane model derived in (8) is the surface Helmholtz energy $\varphi(J)$, which regulates the in-plane stretching behavior of the membrane and can describe the phase transition phenomena taking place in lipid bilayers (Fig. 2).

The lipid bilayer is formed by two facing monolayers of lipid molecules, each of which is characterized by a hydrophilic head and a hydrophobic tail. Depending on temperature and on the surrounding conditions, each lipid molecule of the bilayer admits an ordered state (L_o), where the hydrophobic tail appears straightened and taller, and a disordered state (L_d), where the tail appears curly and shortened.

By raising temperature, the hydrocarbon tails of the phospholipid molecules undergo a significant thickness reduction from the liquid ordered phase L_o to the liquid disordered phase L_d: This justifies the choice of the bilayer current thickness h as a good coarse-grained order parameter for the description of the $L_o - L_d$ transition. Furthermore, due to the quasi-incompressibility condition (5), also the areal stretch J can be used as order parameter. Both choices have been widely adopted in literature (see, e.g., Goldstein and Leibler 1989; Owicki and McConnell 1979; Sackmann 1995).

The experimental evidence clearly shows that for a given chemical composition there may exist a temperature range where the L_o and L_d phases coexist, organizing themselves in domains called *rafts*. In closed membranes, these domains are typically detectable by curvature inhomogeneities, reflecting the occurrence of different bending rigidities (Baumgart et al.

2003). The expressions (12) for the bending rigidities show how the order–disorder transition, described by the stretching energy $\varphi(J)$, is connected with bending behavior of the membrane. Furthermore, as we will prove, the stretching energy density $\varphi(J)$ also determines the line tension occurring at the phase boundary.

A classical method to determine $\varphi(J)$ in the framework of the $L_o - L_d$ transition is the construction of an appropriate phenomenological Landau expansion of the stretching free energy in powers of the current thickness h, or in powers of the areal stretch J (see, e.g., Goldstein and Leibler 1989; Komura et al. 2004; Owicki and McConnell 1979). The advantage of the Landau expansion is that its phenomenological parameters can be related to measurable quantities, such as the transition temperature, the latent heat, and the order parameter jump (see Goldstein and Leibler 1989 and the treatise Sackmann 1995 for a detailed discussion).

By assuming that for a fixed temperature the membrane natural configuration $\mathscr{B}_0$ coincides with the flat, ordered L_o phase, in which $J = J_o = 1$, the stretching energy is chosen in the form

$$\varphi(J) = a_0 + a_1 J + a_2 J^2 + a_3 J^3 + a_4 J^4, \tag{13}$$

where the phenomenological parameters a_i $(i = 0, \ldots, 4)$ depend in general on temperature and chemical composition. In the lack of specific experimental data and in order to show the numerical feasibility of the model, we calibrate these parameters on the basis of the experimental estimates provided by Goldstein and Leibler (1989). These experimental data have been also used in Komura et al. (2004) to describe the temperature-driven order–disorder transition in lipid bilayers. For a temperature $T \sim 30°$, we find

$$\begin{aligned} a_0 = 2.03, \quad a_1 = -7.1, \quad a_2 = 9.23, \\ a_3 = -5.3, \quad a_4 = 1.13, \end{aligned} \tag{14}$$

dimensionally expressed in $[J][m]^{-2}$. It is worth pointing out that this specific choice is merely indicative and is meant to show the numerical feasibility of the current approach. Clearly, in order to get a finer description of the membrane behavior, specific data on the bilayer chemical composition and the temperature are required; these measurable data can be incorporated in our approach (see Deseri et al. 2008 for details) although we neglect them in the subsequent analysis.

4 Order–disorder transition in a planar membrane

The study of the equilibrium problem for a planar lipid membrane described by the energy (13) with the phenomenological parameters given by (14) permits to elucidate the occurrence of thickness inhomogeneities in the membrane and allows one to calculate the corresponding bending rigidities, the shape of the boundary layer between the ordered and disordered phases, and to determine the corresponding line tension.

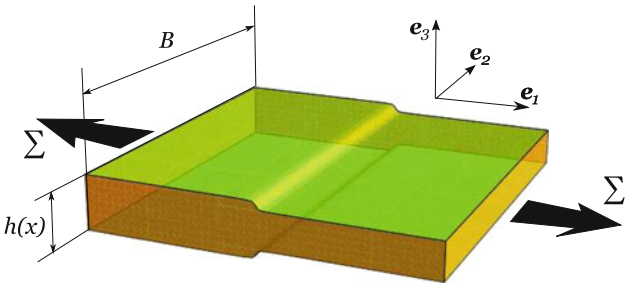

Fig. 3 A scheme of the problem here considered, representing the smooth transition from the thicker L_o domain to the thinner L_d domain under a traction Σ in the $\boldsymbol{e}_1$ direction

The analysis carried out in this work should be intended as a first step of a more general problem, where the order–disorder phenomena take place on a closed, curved biological membrane in aqueous solution. Aside analytical difficulties arising from the geometry, in that case there are further sources of complication arising from the nature of boundary conditions, which may be represented by the external control of the osmotic pressure or of the enclosed volume or mass (see, e.g., De Tommasi et al. 2013a).

Following Coleman and Newman (1988), we consider a membrane that in the reference configuration $\mathscr{B}_0$ has the form of a thin plate of homogeneous thickness h_0 (direction $\boldsymbol{e}_3$), width B (direction $\boldsymbol{e}_2$), and length L (direction $\boldsymbol{e}_1$)—see Fig. 3. The reference mid-surface Ω of the membrane corresponds to $z = 0$, and its lateral edges are defined by $x = \pm L/2$ and $y = \pm B/2$.

The three-dimensional membrane deformation is further restricted with respect to (4), according to

$$\boldsymbol{f}(\boldsymbol{x}) = g(x)\boldsymbol{e}_1 + y\boldsymbol{e}_2 + z\phi(x)\boldsymbol{e}_3 \tag{15}$$

so that the width B is kept constant. Calculating the deformation gradient of $\boldsymbol{f}$, we get

$$\mathbf{F} = \nabla \boldsymbol{f} = \begin{bmatrix} g_x & 0 & 0 \\ 0 & 1 & 0 \\ z\phi_x & 0 & \phi \end{bmatrix}, \tag{16}$$

where the subscript x denotes differentiation with respect to x. The displacement component along $\boldsymbol{e}_1$ is $u(x) = g(x) - x$. After setting

$$\lambda(x) = g_x(x) \tag{17}$$

for the stretch in direction $\boldsymbol{e}_1$, we have $\det \mathbf{F} = \lambda\phi$ and $J = \lambda$. The incompressibility condition then implies $\phi = \lambda^{-1}$, so that the membrane deformation is completely determined by λ.

Denoting by $\hat{\lambda}$ the spatial description of λ, so that the composition $\hat{\lambda} = \lambda \circ g^{-1}$ holds, observe that the gradient

terms occurring in (8)

$$||\text{grad}_\omega \hat{J}||^2 = ||\text{grad}_\omega \hat{\lambda}||^2 = \lambda_x^2 \lambda^{-2}, \tag{18}$$

so that the energy per reference area (8) reduces to

$$\psi(\lambda, \lambda_x) = \varphi(\lambda) + \frac{h_0^2}{24}\lambda^{-5}\varphi'(\lambda)\lambda_x^2 \tag{19}$$

where, since here $J = \lambda$, we denote $' = d/d\lambda$. Following Coleman and Newman (1988), we introduce the functions

$$\gamma(\lambda) = -\frac{h_0^2}{12}\lambda^{-5}\varphi'(\lambda), \quad \beta(\lambda) = \frac{1}{2}\gamma'(\lambda), \tag{20}$$

so that the surface energy density can be recast as

$$\psi(\lambda, \lambda_x) = \varphi(\lambda) - \frac{1}{2}\gamma(\lambda)\lambda_x^2. \tag{21}$$

With γ a negative constant rather than a function of λ, the energy functional (21) falls within the framework of Cahn–Hilliard models of phase transitions in fluids. This model has received extensive attention in literature (see, e.g., Alberti 2000), and it is based on the fundamental assumption that $\gamma < 0$, which is required in order to penalize the spatial inhomogeneities of λ.

With γ a function of λ, the form of (21) is consistent with the energy density deduced in Coleman and Newman (1988) for the drawing of polymeric films. As well as in the Cahn–Hilliard model, the condition $\gamma(\lambda) < 0$ is necessary in order to guarantee a physically meaningful behavior. This condition is actually satisfied by the energy density (13).

We assume that the membrane is under the action of opposite tractions of intensity Σ (force per reference length) on the edges $x = \pm L/2$, although the case for which the end displacements are controlled may be treated in an analogous way (see, e.g., Triantafyllidis and Bardenhagen 1993). Due to the presence of nonlocal terms λ_x in the constitutive response of the bar, it is in general necessary to introduce *hyper-tractions* Γ which perform work corresponding to changes of the displacement gradient u_x (Puglisi 2007). With these positions, the mechanical work on the bar can be written as

$$\mathscr{W}(u, u_x) = B\left[\Sigma u\right]_{-L/2}^{+L/2} + B\left[\Gamma u_x\right]_{-L/2}^{+L/2}. \tag{22}$$

The total potential energy corresponding to a deformation g is then

$$\mathscr{E}(\boldsymbol{g}) = B\int_{-L/2}^{L/2} \psi(\lambda, \lambda_x)\, dx - \mathscr{W}(u, u_x). \tag{23}$$

We now impose the stationarity of (23) in order to find the Euler–Lagrange equations and boundary conditions. To this end, introduce a perturbation $\eta(x)$ and let

$$g_\varepsilon(x) := g(x) + \varepsilon\eta(x). \tag{24}$$

By standard calculations based on the arbitrariness of η, the vanishing of the first variation $\delta E = dE(g_\varepsilon)/d\varepsilon|_{\varepsilon=0}$ of (23) gives the following Euler–Lagrange equation,

$$\Sigma = \varphi'(\lambda) + \beta(\lambda)\lambda_x^2 + \gamma(\lambda)\lambda_{xx} = \text{const.}, \tag{25}$$

which must be satisfied for all x in $(-L/2, L/2)$, and the boundary conditions

$$\left[\Gamma + \gamma(\lambda)\lambda_x\right]_{-L/2} = \left[\Gamma + \gamma(\lambda)\lambda_x\right]_{+L/2} = 0. \tag{26}$$

Here we are interested in describing the localization of deformations leading to the possible coexistence of a thicker region (the ordered, L_o phase) and a thinner region (the disordered, L_d phase), connected by a transition boundary layer.

Effects arising from finite boundaries will not be considered in this analysis so that, consistently with Coleman and Newman (1988), we take L unbounded, with $-\infty < x < \infty$. Furthermore, we assume $\Gamma = 0$ at the bar ends, so that (26) imposes that λ_x must tend to zero as x tends to $\pm\infty$.

Each nontrivial bounded solution of (25) obeys the equation

$$x - \bar{x} = \int_{\lambda(\bar{x})}^{\lambda(x)} \left(\frac{-2}{\gamma(\lambda)} \int_{\lambda_a}^{\lambda} \left[\varphi'(\zeta) - \Sigma\right] d\zeta \right)^{-\frac{1}{2}} d\lambda, \tag{27}$$

where $\bar{x}$ is arbitrary and where λ_a is the value of λ at a place or limit where $\lambda_x = 0$. The derivation of (27) is classical and can be found in Coleman and Newman (1988).

For $\gamma(\lambda) < 0$ and depending on the values of the applied traction $\Sigma > 0$, the nontrivial, bounded solutions of (25) have been completely characterized in Coleman and Newman (1988). According to the number of points where $\lambda_x = 0$, these must fall in one of the following classes:

1. λ is strictly monotone, if $\lambda_x \neq 0$ for any finite point;
2. λ exhibits a *bulge* or a *neck*, if there exists precisely one value of x where $\lambda_x = 0$ in which $\lambda(x)$ attains a minimum or a maximum, respectively;
3. λ is periodic, if there is more than one finite value of x at which $\lambda_x = 0$.

Strictly, monotone solutions are of specific interest of this work. These are characterized by

$$\begin{aligned} &\lim_{x\to-\infty} \lambda = \lambda_*, \qquad \lim_{x\to+\infty} \lambda = \lambda^* \\ &\lim_{x\to\pm\infty} \lambda_x = 0, \qquad \lim_{x\to\pm\infty} \lambda_{xx} = 0. \end{aligned} \tag{28}$$

The analysis in Coleman and Newman (1988) shows that these can be attained provided that the applied traction equals the Maxwell stress Σ_M, which is determined by the equal area rule

$$\int_{\lambda_*}^{\lambda^*} \left[\varphi'(\lambda) - \Sigma_M\right] d\lambda = 0, \tag{29}$$

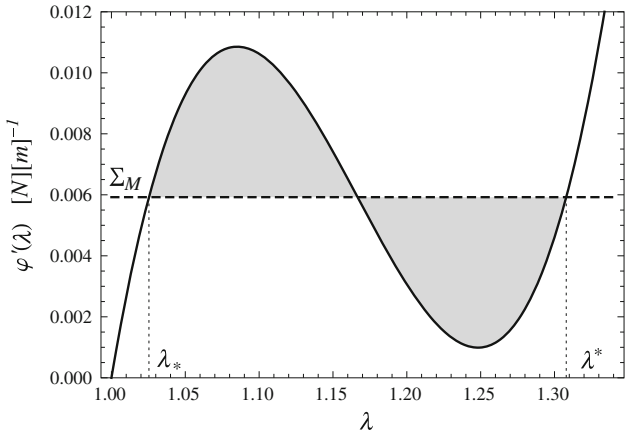

Fig. 4 The function $\varphi'(J)$ and the value of the Maxwell stress $\Sigma_M = 5.92\,\text{mN m}^{-1}$, resulting from the equal area rule (*gray regions*)

with $\Sigma_M = \varphi'(\lambda_*) = \varphi'(\lambda^*)$—see Fig. 4. These solutions are uniquely determined to within a reflection or translation. The monotonicity of $\lambda(x)$ permits to determine x as a function of λ from (27), with $\lambda_a \equiv \lambda_*$ and $\bar{x}$ arbitrary, such that $\lambda_* < \lambda(\bar{x}) < \lambda^*$.

For the specific energy (13), it results (see Fig. 4)

$$\Sigma_M = 5.92\,\text{mN m}^{-1}, \quad \lambda_* = 1.025, \quad \lambda^* = 1.308. \tag{30}$$

Assuming $h_0 = 45.5\,\text{Å}$ for the reference thickness of the ordered phase (adapted from Goldstein and Leibler 1989) and by making use of (13,20), the numerical integration of (27) gives the function $\lambda(x)$ within the range (λ_*, λ^*).

The solution and the thickness profile inside the boundary layer are depicted in Fig. 5. As $\lambda(x)$ is strictly monotone, the limit values (λ_*, λ^*) are attained at infinity, but the obtained solution shows a strong localization of deformation inside a boundary layer of length $\simeq 15\,\text{Å}$, where the transition from λ_* to λ^* is almost completely concentrated. As it was expected, the length of the boundary layer and the membrane thickness have the same order of magnitude. This estimate of the length of the boundary layer is in good agreement with other theoretical estimates, in particular we recall (Akimov et al. 2003).

Outside of the boundary layer, the stretch is practically constant, with the thickness amounting to $44.4\,\text{Å} \simeq h_* = h_0/\lambda_*$ and to $34.8\,\text{Å} \simeq h^* = h_0/\lambda^*$.

The two domains where the stretch is practically equal to λ_* and λ^* are the L_o and L_d phases, respectively. From (25), the Piola stress (per reference length) in both phases is Σ_M, whereas the Cauchy stress (per current length) in the two domains amounts to

$$\begin{aligned} t^{L_o} &= t_* = \Sigma_M \lambda_* = 6.07\,\text{mN m}^{-1} \\ t^{L_d} &= t^* = \Sigma_M \lambda^* = 7.74\,\text{mN m}^{-1}. \end{aligned} \tag{31}$$

These values of surface tension are merely indicative, since these are based on the special form of $\varphi(J)$ assumed in (13); nevertheless, these values are coherent with the experimental estimates of surface stress in ordered and disordered domains (see, e.g., Semrau et al. 2008), according to which the stress in the disordered phase is sensibly higher than in the ordered phase. Also, observe that the calculated values of surface stress are compatible with the range of physiologically accepted values of membrane tension (0–15 mN m^{-1}).

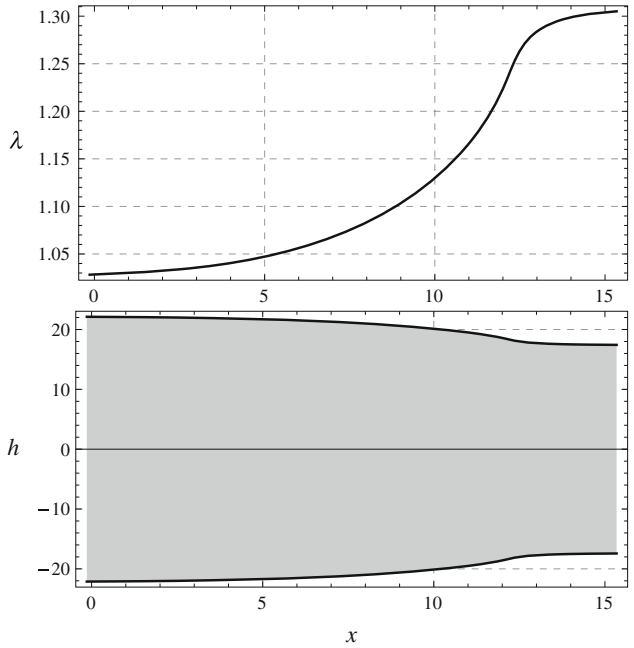

Fig. 5 The function $\lambda(x)$ (*up*) and the thickness profile $h(x)$ (*down*) in correspondence of $\Sigma = \Sigma_M$. Lengths expressed in Å

Furthermore, our estimates are consistent with the analysis performed in Reddy et al. (2012), where the role played by surface tension in changes of the lipid conformational order has been investigated.

5 Energy minimization and line tension

In this section, we show that the thickness profile determined in (27) is a global minimizer of the total potential energy $\mathscr{E}$ in the class of smooth solutions which fulfill the boundary conditions (28). Furthermore, we show that this specific profile can be used in order to deduce an optimal value of the line tension between the ordered and disordered phases.

The analysis of phase coexistence in fluid systems classically follows two different theories: the *gradient theory* and the *sharp interface theory*.

According to the gradient theory, the order parameter J is not allowed to undergo discontinuities and the analysis is based on the minimization of the total potential energy

$$\mathscr{E} = \int_\Omega \left[\varphi(J) + \alpha(J)||\text{grad}_\omega \hat{J}||^2\right] \text{d}\Omega - \mathscr{W}. \tag{32}$$

According to the sharp interface theory, the order parameter J is allowed to undergo discontinuities and the total potential energy takes the form

$$\mathscr{F} = \int_{\Omega} \varphi(J)\,\mathrm{d}\Omega + \sigma\,\ell([\![J]\!]) - \mathscr{W}, \tag{33}$$

where σ is the *line tension* (dimensionally, a force) between the two phases and where ℓ is the length of the interface (a jump set, properly) across which J may experience discontinuities.

A rigorous analysis shows that these two approaches are intimately connected, since it can be proved that minimizers of $\mathscr{E}$ converge (in a suitable sense) to minimizers of $\mathscr{F}$ (see, e.g., Alberti 2000 for a detailed discussion of this topic). Here, we deduce an optimal value of the line tension by evaluating the global minima of the potential energy $\mathscr{E}$ in the class of solutions which fulfill the boundary conditions (28).

As first thing, observe that by the identity $u_x(x) = \lambda(x) - 1$ the work term can be recast as follows

$$\mathscr{W} = B \int_{-L/2}^{L/2} \Sigma_M \lambda\,\mathrm{d}x - B\Sigma_M L. \tag{34}$$

Observe that $\varphi(\lambda_*) - \Sigma_M\lambda_* = \varphi(\lambda^*) - \Sigma_M\lambda^*$, so it makes sense to introduce the function $\tilde{\varphi}(\lambda) = \varphi(\lambda) + c$, where

$$c = \Sigma_M\lambda_* - \varphi(\lambda_*) = \Sigma_M\lambda^* - \varphi(\lambda^*), \tag{35}$$

so that

$$\tilde{\varphi}(\lambda_*) - \Sigma_M\lambda_* = \tilde{\varphi}(\lambda^*) - \Sigma_M\lambda^* = 0. \tag{36}$$

Also, observe that for $\lambda \neq \lambda_*$ and $\lambda \neq \lambda^*$, it results

$$\tilde{\varphi}(\lambda) - \Sigma_M\lambda \geq 0. \tag{37}$$

First, make reference to the gradient approach. Following the discussion in Sect. 4, assume that the bar is subject to a traction Σ_M, that $\lambda(x)$ is monotone in the interval $(-L/2, L/2)$, that $\lambda \to \lambda_*$ as $x \to -L/2$, and that $\lambda \to \lambda^*$ as $x \to L/2$.

Since L is unbounded, we take in consideration the total potential energy per length unit $\mathscr{E}/L$. By making use of (34,36), for any profile which satisfies the boundary conditions (28), it results

$$\frac{\mathscr{E}}{L} = \frac{B}{L}\int_{-L/2}^{L/2}\left[(\tilde{\varphi}(\lambda) - \Sigma_M\lambda) - \frac{\gamma(\lambda)}{2}\lambda_x^2\right]\mathrm{d}x + d, \tag{38}$$

where $d = B(\Sigma_M - c)$ is a constant.

We now prove that the profile determined in (27) by the stationarity condition is a minimizer of $\mathscr{E}/L$. The argument of the minimization procedure is inspired by the approach followed in Alberti (2000). By $\tilde{\varphi}(\lambda) - \Sigma_M\lambda \geq 0$, by $-\gamma(\lambda)\lambda_x^2 \geq 0$, by the monotonicity of λ, and by the inequality $a^2 + b^2 \geq 2ab$, it results that the following inequality holds:

$$\frac{\mathscr{E}}{L} \geq \frac{B}{L}\int_{\lambda_*}^{\lambda^*}\sqrt{-2\gamma(\lambda)\,(\tilde{\varphi}(\lambda) - \Sigma_M\lambda)}\,\mathrm{d}\lambda + d, \tag{39}$$

equality holding if and only if $a = b$, that is,

$$\tilde{\varphi}(\lambda) - \Sigma_M\lambda = -\frac{\gamma(\lambda)}{2}\lambda_x^2. \tag{40}$$

At this point, consider that by (36),

$$\tilde{\varphi}(\lambda) - \Sigma_M\lambda = \int_{\lambda_*}^{\lambda}\left(\varphi'(\zeta) - \Sigma_M\right)\mathrm{d}\zeta \tag{41}$$

so that by integration of (40), we obtain exactly the profile determined in (27). Thus, we have proved that in the class of profiles which satisfy the limit boundary conditions (28), the following minimum of the total potential energy is attained

$$\min\left(\frac{\mathscr{E}}{L}\right) = \frac{B}{L}\int_{\lambda_*}^{\lambda^*}\sqrt{-2\gamma(\lambda)\,(\tilde{\varphi}(\lambda) - \Sigma_M\lambda)}\,\mathrm{d}\lambda + d, \tag{42}$$

provided $\lambda(x)$ is given by (27).

Make now reference to the sharp interface approach. More in detail, consider a configuration characterized by $\lambda = \lambda_*$ for $x < x_0$ and $\lambda = \lambda^*$ for $x > x_0$, so that in $x = x_0$ there is a sharp transition. Here, x_0 is an arbitrary finite point, and also in this case, the bar is subjected to a traction Σ_M. In this configuration, a short calculation reveals that the total potential energy (33) per length unit is

$$\frac{\mathscr{F}}{L} = \frac{B}{L}\sigma + d. \tag{43}$$

Finally, the comparison of (38), (42), and (43) permits to identify the line tension of the sharp interface model with

$$\sigma := \int_{\lambda_*}^{\lambda^*}\sqrt{-2\gamma(\lambda)\,(\tilde{\varphi}(\lambda) - \Sigma_M\lambda)}\,\mathrm{d}\lambda. \tag{44}$$

With reference to the numerical data (14), integration of (44) gives

$$\sigma = 3.88 \times 10^{-13}\,\mathrm{N} \tag{45}$$

which is consistent with the value $9 \pm 0.3 \times 10^{-13}\,\mathrm{N}$ measured in experiments with specific reference to the order–disorder transition (see, e.g., Baumgart et al. 2003; Semrau et al. 2008).

Our results regarding the thickness profile and the line tension are also consistent with other theoretical analysis for lipid mono- and bilayers, which are based on the competition of stretching and *tilt* elasticity—which is due to the fact that lipid molecules can deviate from the mid-surface normal (see, e.g., Akimov et al. 2003; Hamm and Kozlov 2000).

According to our model characterized by a restricted kinematics (4) which does not allow tilt deformations, the role of tilt elasticity is here played by the nonlocal modulus $\alpha(J)$.

6 Elastic moduli

In this section, we deduce the numerical values of the elastic moduli in a phase-separated planar membrane in which a liquid ordered phase $L_o(\lambda = \lambda_*)$ and a liquid disordered phase L_d $(\lambda = \lambda^*)$ coexist under a traction Σ_M.

Area compressibility modulus. With reference to the stress $\Sigma = \varphi'(\lambda)$, which is expressed as a force per unit length in the reference configuration, we can define the tangent area compressibility modulus as

$$K_A(\lambda) := \varphi''(\lambda). \tag{46}$$

Obviously, since $\varphi(\lambda)$ is not quadratic, the value of K_A is not constant. For the specific choice of φ in (13), the tangent value of K_A in the ordered and disordered phases is

$$K_A(\lambda_*) = K_A(\lambda^*) = 181\,\mathrm{mN\,m^{-1}}. \tag{47}$$

When this modulus is calculated in the origin $(J = 1)$, we obtain

$$K_A(1) = 288\,\mathrm{mN\,m^{-1}}, \tag{48}$$

showing a softening behavior. These values are consistent with the existing experimental measurements. Also, observe that in the elastic range of the L_o phase, the maximum areal stretch is $\delta A/A_0 = \lambda_* - 1 = 0.025$, which is consistent with the critical rupture stretch of lipid bilayers (Sackmann 1995).

Bending rigidity. Regarding the bending rigidity, the expression $(12)_1$ is in good agreement with the theoretical and experimental estimates available in literature (see, e.g., Bermúdez et al. 2004; Evans 1974; Norouzi et al. 2006; Pan et al. 2009; Rawicz et al. 2000). For the numerical values in the ordered and disordered phases at equilibrium, we obtain

$$\kappa^{L_o} = \kappa(\lambda_*) = 6.10 \times 10^{-19}\,\mathrm{J}, \tag{49}$$

$$\kappa^{L_d} = \kappa(\lambda^*) = 4.78 \times 10^{-19}\,\mathrm{J}, \tag{50}$$

which are consistent with experimentally measured values. More in detail, the ratio of these rigidities is

$$\frac{\kappa^{L_o}}{\kappa^{L_d}} = 1.27 \tag{51}$$

which is in perfect agreement with the experimental measurements (see, e.g., Baumgart et al. 2003; Chu et al. 2005; Semrau et al. 2008) according to which the ordered phase has a higher bending rigidity.

Gaussian rigidity. The calculation of this rigidity is crucially based on the spontaneous curvature of each monolayer (Hu et al. 2012; Siegel and Kozlov 2004), whereas the model proposed in Deseri et al. (2008), Zurlo (2006) does not take in consideration this effect. Our numerical estimates, based on the assumption that each monolayer has zero spontaneous curvature, give values of κ_G of order 10^{-21} J, which is two orders of magnitude lower than the current theoretical and experimental estimates (see, e.g., Norouzi et al. 2006; Semrau et al. 2008). In order to overcome this limit of our model and in order to enlighten the role of spontaneous curvature within the framework of asymptotic theories for thin membranes, a refinement of the model presented in Deseri et al. (2008), Zurlo (2006) is currently in preparation.

Notwithstanding, even under the limiting assumption of neglecting spontaneous curvature, we observe that from $(10)_2$ and (11), it results

$$\alpha(J) = \frac{k_G(J)}{2J^2}, \tag{52}$$

which discloses a possible connection between variations of the Gaussian rigidity and the order–disorder transition. Indeed, it is well known that, by making use of the Gauss–Bonnet Theorem, the role of the Gaussian rigidity k_G emerges in correspondence of the boundaries of the regions in which J is constant, that is, the phase boundaries between the L_o and the L_d phases; on the other side, the role of the function $\alpha(J)$ emerges in determining the line tension inside the boundary layer, as it was discussed in Sect. 5. Both these issues are consistent with the relation established in Eq. (52).

This issue will be further explored in a forthcoming work where the role of spontaneous curvature has been taken in consideration.

Acknowledgments G. Zurlo gratefully acknowledges the European Project INdAM-COFUND. L. Deseri thanks the University of Trento for partial financial support, the Department of Mathematical Sciences and Center for Nonlinear Analysis through the NSF Grant No. DMS-0635983.

References

Agrawal A, Steigmann DJ (2008) Coexistent fluid-phase equilibria in biomembranes with bending elasticity. J Elast 93(1):63–80

Agrawal A, Steigmann DJ (2009) Modeling protein-mediated morphology in biomembranes. Biomech Mod Mechanobiol 8(5):371–379

Akimov SA, Kuzmin PI, Zimmerberg J, Cohen FS, Chizmadzhev YA (2003) An elastic theory for line tension at a boundary separating two lipid monolayer regions of different thickness. J Electroanal Chem 564:13–18

Alberti G (2000) Variational models for phase transitions. An approach via Γ-convergence, published in L. Ambrosio, N. Dancer: calculus of variations and partial differential equations. In: Buttazzo G et al (eds) Topics on geometrical evolution problems and degree theory. Springer, Berlin, pp 95–114

Baesu E, Rudd RE, Belak J, McElfresh M (2004) Continuum modeling of cell membranes. Int J Nonlinear Mech 39:369–377
Baumgart T, Webb WW, Hess ST (2003) Imaging coexisting domains in biomembrane models coupling curvature and line tension. Nature 423:821–824
Baumgart T, Das S, Webb WW, Jenkins JT (2005) Membrane elasticity in giant vesicles with fluid phase coexistence. Biophys J 89:1067–1080
Bermúdez H, Hammer DA, Discher DE (2004) Effect of bilayer thickness on membrane bending rigidity. Langmuir 20:540–543
Biscari P, Bisi F (2002) Membrane-mediated interactions of rod-like inclusions. Eur Phys J E 7:381–386
Canham PB (1970) The minimum energy of bending as a possible explanation of the biconcave shape of the human red blood cell. J Theor Biol 26:61–80
Chen L, Johnson ML, Biltonen RL (2001) A macroscopic description of lipid bilayer phase transitions of mixed-chain phosphatidylcholines: chain-length and chain-asymmetry dependence. Biophys J 80:254–270
Choksi R, Morandotti M, Veneroni M (2012) Global minimizers for axisymmetric multiphase membranes. ESAIM: COCV. doi:10.1051/cocv/2012042
Chu N, Kucerka N, Liu Y, Tristram-Nagle S, Nagle JF (2005) Anomalous swelling of lipid bilayer stacks is caused by softening of the bending modulus. Phys Rev E 71:041904
Coleman BD, Newman DC (1988) On the rheology of cold drawing. I. Elast Mater J Polym Sci Part B Polym Phys 26:1801–1822
Das S, Tian A, Baumgart T (2008) Mechanical stability of micropipet-aspirated giant vesicles with fluid phase coexistence. J Phys Chem B 112:11625–11630
De Tommasi D, Puglisi G, Zurlo G (2011) Compression-induced failure of electroactive polymeric thin films. Appl Phys Lett 98:123507. doi:10.1063/1.3568885
De Tommasi D, Puglisi G, Zurlo G (2012) Taut states of dielectric elastomer membranes. Int J Non-linear Mech 47:355–361. doi:10.1016/j.ijnonlinmec.2011.08.002
De Tommasi D, Puglisi G, Zurlo G (2013a) Inhomogeneous spherical configurations of inflated membranes. Continuum Mech Thermodyn 25(2):197–206
De Tommasi D, Puglisi G, Zurlo G (2013b) Electromechanical instability and oscillating deformations in electroactive polymer films. Appl Phys Lett 102:011903. doi:10.1063/1.4772956
Deseri L, Owen DR (2003) Toward a field theory for elastic bodies undergoing disarrangements. J Elast 70(1):197–236. doi:10.1023/B:ELAS.0000005584.22658.b3
Deseri L, Owen DR (2010) Submacroscopically stable equilibria of elastic bodies undergoing disarrangements and dissipation. Math Mech Solids 15(6):611–638
Deseri L, Owen DR (2012) Moving interfaces that separate loose and compact phases of elastic aggregates: a mechanism for drastic reduction or increase in macroscopic deformation. Continuum Mech Thermodyn. doi:10.1007/s00161-012-0260-y
Deseri L, Piccioni MD, Zurlo G (2008) Derivation of a new free energy for biological membranes. Continuum Mech Thermodyn 20(5):255–273. doi:10.1007/s00161-008-0081-1
Deseri L, Healey TJ, Paroni R Material gamma-limits for the energetics of biological in-plane fluid films in preparation—private communication
Evans EA (1974) Bending resistance and chemically induced moments in membrane bilayers. Biophys J 14:923–931
Goldstein RE, Leibler S (1989) Structural phase transitions of interacting membranes. Phys Rev A 40(2):1025–1035
Hamm M, Kozlov MM (2000) Elastic energy of tilt and bending of fluid membranes. Eur Phys J E 3:323–335
Helfrich W (1973) Elastic properties of lipid bilayers: theory and possible experiments. Z Naturforsch [C] 28(11):693–703
Honerkamp-Smith AR, Cicuta P, Collins MD, Veatch SL, den Nijs M, Schick M, Keller SL (2008) Line tensions, correlation lengths, and critical exponents in lipid membranes near critical points. Biophys J 95:236–246
Hu M, Briguglio JJ, Deserno M (2012) Determining the Gaussian curvature modulus of lipid membranes in simulations. Biophys J 102:1403–1410
Iglic A (ed) (2012) Advances in planar lipid bilayers and liposomes, 1st ed, vol 15. Academic Press, London
Jenkins JT (1977) Static equilibrium configurations of a model red blood cell. J Math Biol 4(2):149–169
Komura S, Shirotori H, Olmsted PD, Andelman D (2004) Lateral phase separation in mixtures of lipids and cholesterol. Europhys Lett 67(2):321
Lipowsky R (1992) Budding of membranes induced by intramembrane domains. J Phys II France 2:1825–1840
Maleki M, Seguin B, Fried E (2012) Kinematics, material symmetry, and energy densities for lipid bilayers with spontaneous curvature. Biomech Model Mechanobiol. doi:10.1007/s10237-012-0459-7
Norouzi D, Müller MM, Deserno M (2006) How to determine local elastic properties of lipid bilayer membranes from atomic-force-microscope measurements: a theoretical analysis. Phys Rev E 74:061914
Owicki JC, McConnell HM (1979) Theory of protein-lipid and protein-protein interactions in bilayer membranes. Proc Natl Acad Sci USA 76:4750–4754
Pan J, Tristram-Nagle S, Nagle JF (2009) Effect of cholesterol on structural and mechanical properties of membranes depends on lipid chain saturation. Phys Rev E Stat Nonlinear Soft Matter Phys 80:021931
Puglisi G (2007) Nucleation and phase propagation in a multistable lattice with weak nonlocal interactions. Continuum Mech Thermodyn 19:299319
Puglisi G, Zurlo G (2012) Electric field localizations in thin dielectric films with thickness non-uniformities. J Electrost 70:312–316. doi:10.1016/j.elstat.2012.03.012
Rawicz W, Olbrich KC, McIntosh T, Needham D, Evans E (2000) Effect of chain length and unsaturation on elasticity of lipid bilayers. Biophys J 79:328–339
Reddy AS, Toledo Warshaviak D, Chachisvilis M (2012) Effect of membrane tension on the physical properties of DOPC lipid bilayer membrane. Biochem Biophys Acta 1818:2271–2281
Sackmann E (1995) Physical basis of self-organization and function of membranes: physics of vesicles, vol 1, ch 5. In: Lipowsky R, Sackmann E (eds) Handbook of biological physics. Elsevier, Amsterdam, pp 213–303
Semrau S, Idema T, Holtzer L, Schmict T, Storm C (2008) Accurate determination of elastic parameters for multicomponent membranes. PRL 100:088101
Siegel DP, Kozlov MM (2004) The Gaussian curvature elastic modulus of N-monomethylated dioleoylphosphatidylethanolamine: relevance to membrane fusion and lipid phase behavior. Biophys J 87:366–374
Trejo M, Ben Amar M (2011) Effective line tension and contact angles between membrane domains in biphasic vesicles. Eur Phys J E 34(8):2–14
Triantafyllidis N, Bardenhagen S (1993) On higher order gradient continuum theories in nonlinear elasticity derivation from and comparison to the corresponding discrete models. J Elast 33:259–293
Zurlo G (2006) Material and geometric phase transitions in biological membranes, Dissertation for the Fulfillment of the Doctorate of Philosophy in Structural Engineering, University of Pisa, etd-11142006-173408